ELSEVIER

PII: S0032-3861(97)00498-9

Polymer Vol. 39 Nos. 8–9, pp. 1559–1567, 1998

0032-3861/97/$17.00+0.00

Mechanical and wear properties of polymethylmethacrylate and polyvinylidene fluoride blends

Jose L. Garcia[a], Kurt W. Koelling[a,*] and Robert R. Seghi[b]
[a]*Department of Chemical Engineering, The Ohio State University, 140 West 19th Avenue, Columbus, OH 43210, USA*
[b]*College of Dentistry, The Ohio State University, Columbus, OH 43210, USA*
(Received 9 February 1997; revised 5 June 1997)

There are several studies regarding the miscibility of polymethylmethacrylate (PMMA) and polyvinylidene fluoride (PVDF) blends in the molten state along with the rheological properties; however, there is a lack of information regarding the glassy state. The mechanical and wear properties of this system were investigated using both steady and dynamic tests. The results do not follow a simple additive rule of mixtures, but they can be readily explained by the phase morphology of the system. The system is semi-compatible with both an amorphous domain and a crystalline domain. The results for increasing PMMA concentration are: glass transition temperature, T_g (− 34–130°C); storage modulus, E′ (1.1–2.6 GPa); flexural strength, σ_o (75–96 MPa); compressive strength, σ_c (60–120 MPa); and relative wear rate, R_A (0.05–1.8 μm/rev). The amorphous blend had a saturation limit of about 40 wt% PVDF.

(Keywords: PMMA/PVDF blends; mechanical properties)

INTRODUCTION

The use of thermoplastic resins as the matrix phase of dental composites is currently under investigation. Polyvinylidene fluoride (PVDF) is of interest because of its typical fluoropolymer characteristics and its miscibility with polymethylmethacrylate (PMMA), which is commonly used as a dental material.

There have been several studies regarding the miscibility of PMMA and PVDF[1–15]. It is well known that this system is compatible in the molten state for all concentrations. It forms a homogenous phase down to the molecular level over a wide range of temperatures and it is characterised by a lower critical solution temperature which is located well above their decomposition temperatures[1]. A thermodynamic analysis leads to the conclusion that this system should be stable at lower temperatures provided that the blends contain less than ~50 wt% PVDF[2]. PVDF crystallises from the melt at high concentrations, forming a two or three-phase system[2,3]. This is a typical example of a semicompatible blend of a semicrystalline and an amorphous polymer where phase separation occurs by crystallisation of the former.

There have been several reports dealing with the rheological behaviour of the PMMA/PVDF systems in the molten state. Some theoretical models have been proposed in order to describe their behaviour, but there is still some difficulty trying to fit the data[4]. Other reports concerning miscibility also deal with polymer melts or melting point behaviour[4–7]. There are only a limited number of papers that present data on the characteristics of the glassy system[1,2]. One of the problems encountered in the literature is the large discrepancy in the reported values of T_g of the blends. It appears that the differences are caused by the processing methods used, from bulk mixing to solution casting, and the final morphology of the system. However, in most applications, particularly injection molding and compression molding, the main form of processing of parts is by bulk melting of materials. It is in the area of bulk melting that there is a significant lack of data regarding the mechanical and wear characteristics of PMMA/PVDF blends. Thus, the main focus of this paper is to present mechanical and wear data of bulk processed PMMA/PVDF blends and to explain the results from the known morphology.

EXPERIMENTAL

Materials and test specimens

PMMA (M.W. 75 000) and PVDF (M.W. 60 000) in powder form from Polysciences, Inc. were used to prepare the polymer blends. The blends of PMMA/PVDF had compositions of 100/0, 90/10, 75/25, 50/50, 25/75, and 0/100 by weight. Samples were prepared by dry mixing the powders as purchased, without further purification, followed by melting and extrusion. Dry mixing was chosen due to its simplicity and the fact that small samples had to be produced. In addition, dry mixing has been shown to be effective for other polymeric systems[5]. The extruder was designed and built to produce small samples with low polymer requirements on the order of 10 g or less. It basically consisted of a heated reservoir and a plunger for extrusion. Samples were extruded at 400°C as 3.5 mm diameter rods and cooled to room temperature by air convection.

Test specimens for two geometries were prepared from

* To whom correspondence should be addressed

the extruded rods: 3.5 × 6 mm cylinders; and 50 × 5 × 1.7 mm bars, which were compression molded from 50 mm long cylinders. The bars were used to determine the density and the flexural properties of the blends. The small cylinders were used to determine the compressive and the relative wear rates of the blends.

Experimental tests

Several tests were performed in order to study the effect of blend composition on mechanical properties. The composition of the blends was verified by density measurements while the miscibility was verified by T_g measurements. Density was measured by volume displacement and the results were compared to a simple additive rule. The T_g was measured from oscillatory flexural measurements as described below.

Flexural properties were tested in both steady and dynamic mode. The steady test was performed using an Instron (Model 4240) fitted with a 3-point bending geometry with a span of 20 mm. The test bars had the dimensions given above and the Instron was operated at a constant crosshead speed of 0.75 mm/min. The load was recorded as a function of displacement. The flexural strength was defined as either the point where the specimen fractured or the ultimate flexural stress, indicating yield. A Weibull analysis was performed to study the randomness of failure and the maximum stresses and strains were compared to study composition effects.

The dynamic measurements were performed in a Rheometrics Solids Analyzer (RSA II). The geometry used was a 3-point bend with a span of 20 mm, as in the steady mode. The sample dimensions are the same as above. The dynamic tests allowed for the determination of the frequency response for the blends at specific temperatures and for the determination of the T_g from temperature sweeps. Temperature sweeps were performed by applying a strain of 0.5% at a frequency of 10 rad/sec and ramping the temperature at 5°C/min. The dynamic nature of the tests allows for the determination of E′ (storage modulus), E″ (loss modulus), and tan δ (phase shift). Transitions in the matrix are indicated by peaks in the tan δ curves which were used to find the T_g.

The frequency sweeps at different temperatures were used to generate master curves for the blends. It is well known that for compatible materials the master curves are similar to those obtained for random copolymers[16,17]. It follows, then, that the shift factors can be represented by the WLF equation or an Arrehnius type equation, depending on the T_g of the system[18]. Thus, the shift factors were fitted according to the T_g of the blend.

Compressive strength was determined using the Instron with parallel plates for compression of the small cylinders. The crosshead speed was set at 0.75 mm/min and the load was recorded as a function of displacement. The compressive strength was determined at the point of failure which was defined to be the ultimate compressive stress.

The relative abrasive wear tests were performed in the two-body wear device shown in *Figure 1*. Wear was induced by sliding a small cylindrical sample over a diamond disk abrader. The specimens were held in contact with the abrasive diamond surface with a continuous 1.5 N load and traced a circular orbiting pattern around the diamond disk. The contacting surfaces were continuously flushed with copious amounts of room temperature tap water. The change in height was recorded as function of time with an LVDT. In this case the most probable causes

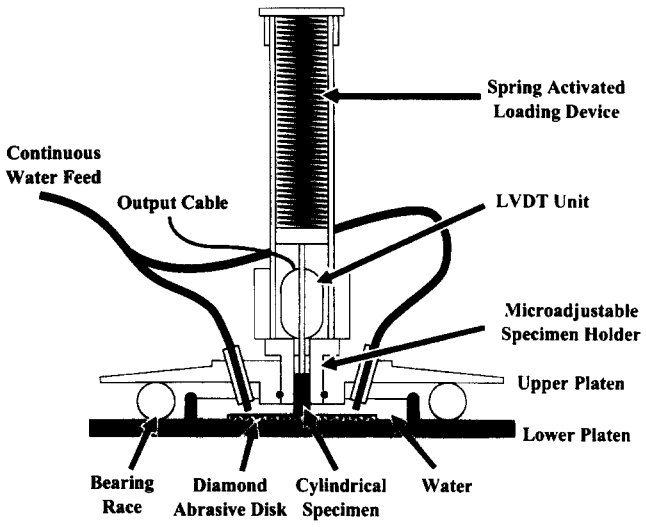

Figure 1 Schematic of two-body wear device used for relative abrasive wear rates

for wear are deformation losses. Plastic flow deformation leads to microcutting, and viscoelastic deformation leads to tearing, cracking, or fatigue[19].

In addition to the mechanical tests, the morphology of the system was studied by transmission electron microscopy (TEM). Samples were prepared by microtoming 90 nm thick sections using a Reichert Ultracut E. These sections were then stained in OsO_4 vapours for approximately 1 h and placed in formula coated grids. A Phillips CM-12 TEM (60 kV) was then used to examine the morphology of the blends.

As indicated previously, these series of tests were aimed at evaluating the effects of blend composition on the mechanical and wear properties. Each of the tests were performed on ten samples.

RESULTS

Figure 2 shows the density (g/cm^3) of the blends as a function of PMMA concentration (wt%). The results for a simple additive rule are also shown in this figure.

The T_g for the blends are shown in *Figure 3*. The data is similar to that obtained by Chuang and Han indicating a large deviation from additivity. It should be noted that the 25/75 (PMMA/PVDF) blend had two transitions, one at −34°C, the T_g for pure PVDF, and the other at about 100°C. All the other samples had only one transition during the temperature sweeps.

Stress–strain data obtained from the Instron, for ten samples of PMMA, is shown in *Figure 4*. Similar data was obtained for all the other compositions. This data was used to calculate the flexural strength and, as can be seen for PMMA, there is significant scatter in the maximum stress before failure. It should be noted, however, that the mode of failure changed as more PVDF was present. The PMMA samples, being brittle, failed by fracturing in all occasions while PVDF samples failed by yielding. The blends went through a transition with more samples yielding instead of fracturing as the PVDF content was increased. The strength was then defined at the point of failure, either by fracture or deformation. *Figure 5* shows the results of a Weibull analysis used to find the characteristic strength, σ_0 (MPa), for the samples. Thus, σ_0 is the variable that should be used for design, since it is directly related to failure. However, σ_0

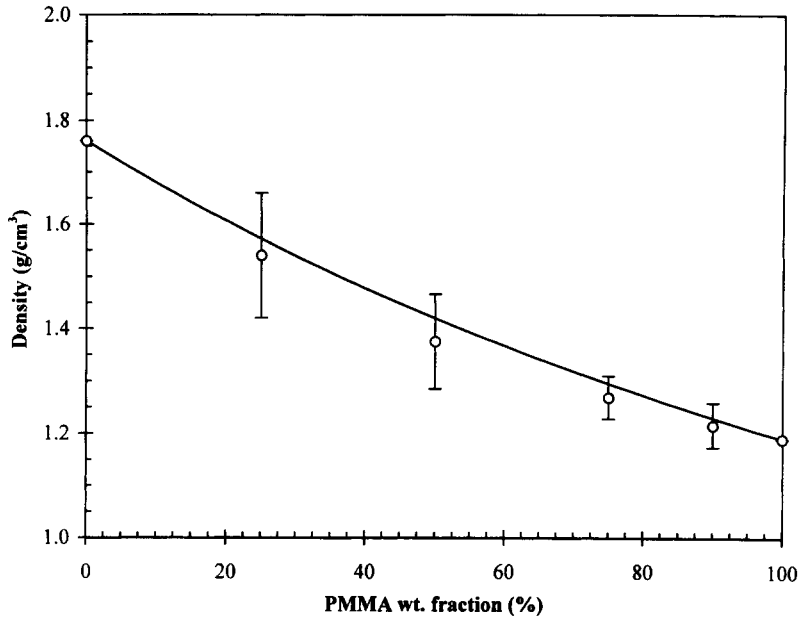

Figure 2 Density of PMMA/PVDF blends as a function of PMMA wt%: (E) experimental data; (———) additive rule

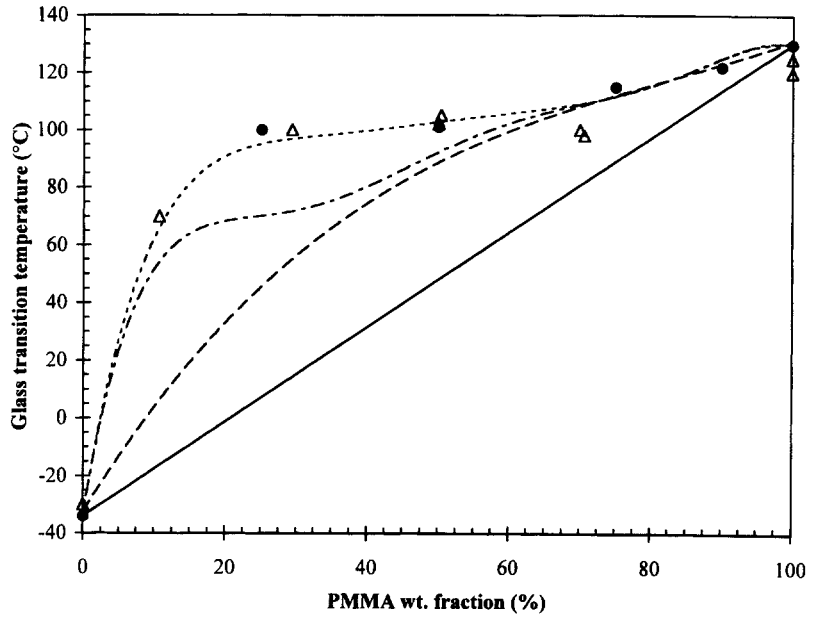

Figure 3 Glass transition temperature of blends as a function of PMMA wt%: (J) experimental data; (C) Chuang and Han[5]; (———) additive rule; (— —) Gordon–Taylor fit; (— - —) modified Gordon–Taylor with Hahn *et al.* data[1]; (- - -) best fit Gordon–Taylor

does not allow for a clear examination of the changes in the matrix. Therefore, in order to see the effects of composition in the matrix, the ultimate flexural strength for the samples and the corresponding strains were plotted (*Figure 6*). While the ultimate flexural strength was easily obtained for the blends (at least one sample underwent yielding before failure), this value was estimated for pure PMMA to be the maximum stress observed in *Figure 4*.

The dynamic flexural modulus, E′ (GPa), at four different frequencies is shown in *Figure 7* as a function of the blend composition. We can see from this figure that the moduli do not follow a simple additivity rule. In addition, the 25/75 (PMMA/PVDF) blend does not seem to fit the trend. A possible explanation is presented in the discussion below. The master curves for the blends are shown in *Figure 8*, where the curves where shifted to 25°C. The parameters for

Table 1 Constants for the different shift factor equations and ranges where they are applicable

WLF parameters

PMMA wt%	C_1 (–)	C_2 (K)	T_g (°C)	Range (°C)	r^2 (–)
0	6.1	31	– 33	– 48–65	0.811
25	14.2	109	100	75–125	0.844
50	8.5	85	101	75–135	0.830
75	11.6	87	115	85–135	0.892
90	8.4	66	122	95–125	0.914
100	7.6	72	130	100–170	0.990

Arrhenius equation parameters

PVDF	E_a (J/mol)	T_R (°C)	Range (°C)	r^2 (–)
	3×10^5	65	65–150	0.967

T_R: Reference temperature; r^2: correlation

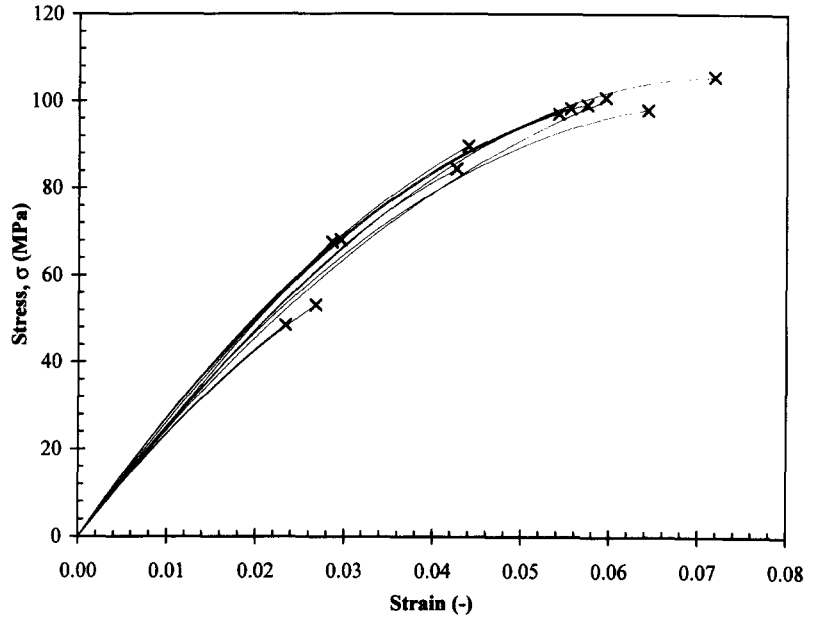

Figure 4 Typical stress–strain data for flexural strength (data for ten samples of PMMA)

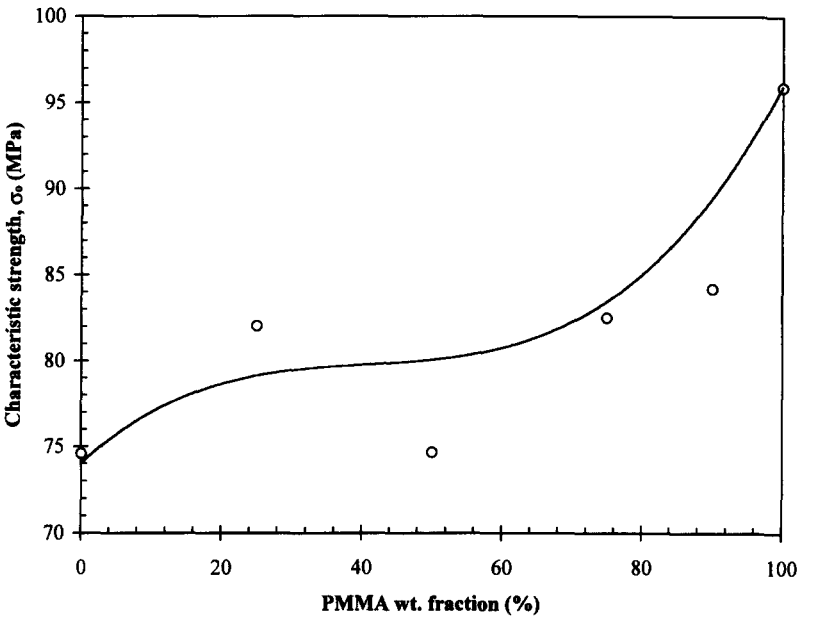

Figure 5 Weibull analysis of flexural strength data

the WLF and Arrhenius fit are shown in *Table 1*. As shown, all the blends had T_g values much higher than room temperature and close to the melting temperature. Thus, a WLF equation was used to describe their behaviour. PVDF, on the other hand, has a T_g of $-34°C$ which is much lower than the melting temperature. Therefore, pure PVDF exhibited both a WLF domain, near T_g, and an Arrhenius domain, above 65°C and below the melting temperature. These two domains are shown in *Figure 9*.

Figure 10 shows the compressive strength, σ_c (MPa), as a function of blend composition. The results agree very well with what is expected from phase morphology and will be discussed later.

The relative abrasive wear rates, R_A (μm/rev), are plotted *versus* blend composition in *Figure 11*. It can be seen that the wear rate increases drastically when the concentration of PMMA increases above 30%.

The TEM pictures showing the morphology of the blends are shown in *Figures 12 and 13*. *Figure 12* shows the morphology for the blends containing 100, 75, and 50 wt% PMMA, while *Figure 13* shows the blends containing 25 and 0 wt% PMMA. It can be seen from these pictures that at concentrations of PVDF less than 50 wt% the blend is homogenous. At higher concentrations, however, one can see the crystalline growth responsible for phase separation. It should be noted that the pure PVDF sample exhibited more crystalline formation than the sample containing 75 wt% PVDF.

DISCUSSION

As indicated above, the mechanical and wear behaviour of PMMA/PVDF blends do not follow a simple rule of

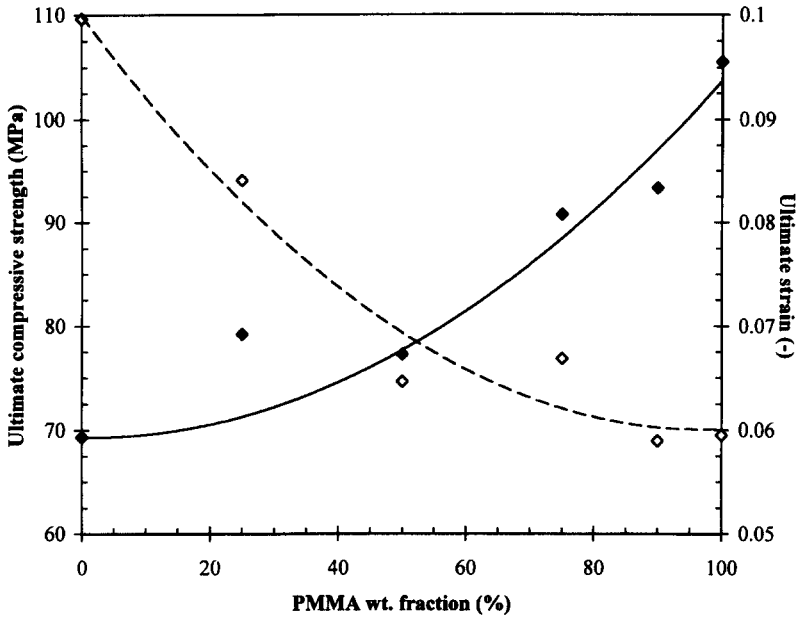

Figure 6 Ultimate strength and strain for the blends: (J) strength; (E) strain

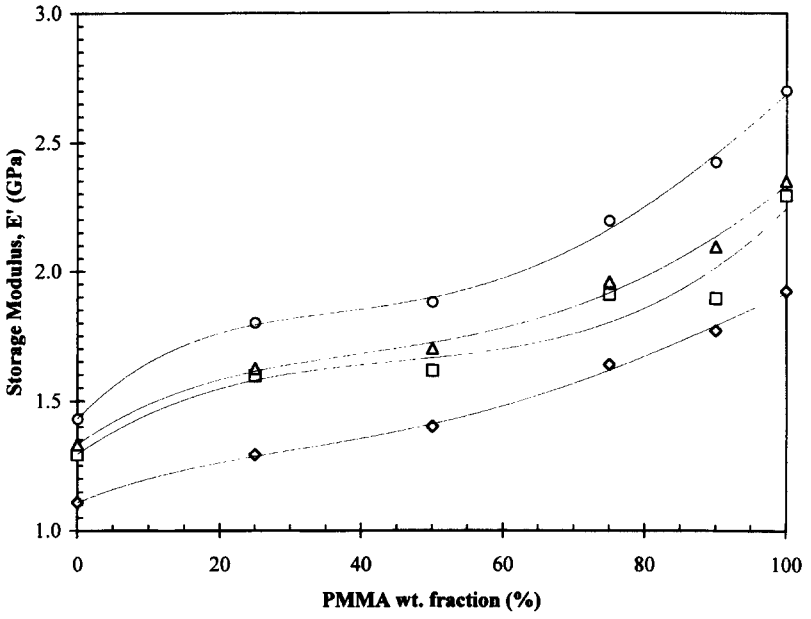

Figure 7 Storage moduli at four frequencies as a function of blend composition: (E) 100 rad/sec; (C) 10 rad/sec; (G) 1.0 rad/sec; (A) 0.1 rad/sec

mixtures. It appears that this behaviour is mainly due to morphological properties of the system. Thus, measurements that are independent of morphology should yield results that agree with the law of mixture. For instance, density measurements agreed very well with the values calculated from the mixing rule:

$$\rho_{blend} = \frac{1}{\frac{\phi_{PMMA}}{\rho_{PMMA}} + \frac{\phi_{PVDF}}{\rho_{PVDF}}}$$

where ϕ's are the weight fractions and ρ's are the densities.

This agreement is in sharp contrast to other measurements where the morphology greatly affects the results. For instance, there is much discrepancy found in literature with respect to the reported values of the T_g of the blends[2,5,7,8,10,12]. These differences seem to be imparted from the different techniques used to prepare the blends, which result in different morphologies in the blends[2]. It has been proposed that the PMMA/PVDF blend system is amorphous for concentrations up to about 50 wt% PVDF. Beyond this value, there is phase separation[1-3]. Several different theories have been developed to explain the morphology of the system at high PVDF concentrations. The system may consist of an amorphous PMMA/PVDF blend and either a crystalline PVDF domain[2,3], or crystalline and amorphous PVDF domains[1]. The important characteristic to keep in mind, however, is that there is an amorphous domain, where the PMMA and PVDF are blended, and a second domain consisting mainly of PVDF. It has been found that T_g data for amorphous mixtures of compatible blends or copolymers fit the Gordon–Taylor equation very closely[2]:

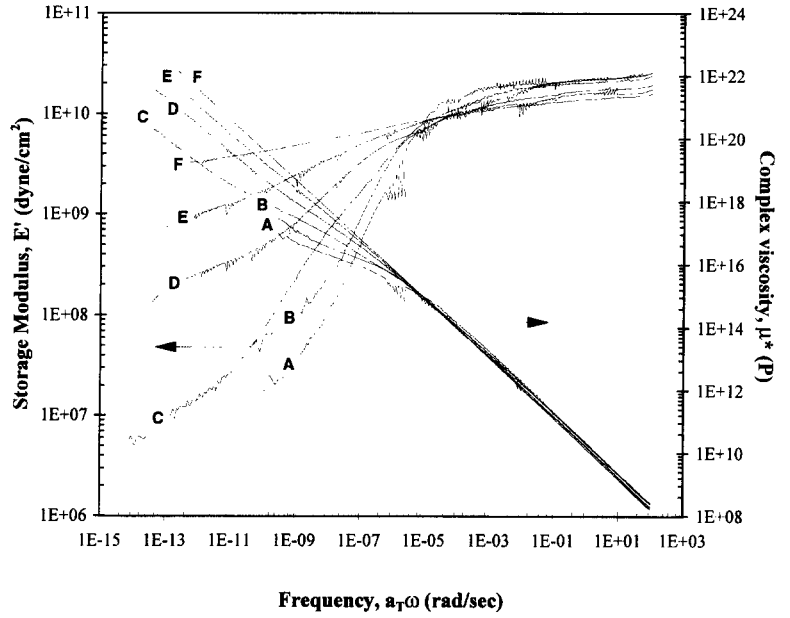

Figure 8 Master curve for the blends, shifted to 25°C: (A) PMMA; (B) 90% PMMA; (C) 75% PMMA; (D) 50% PMMA; (E) 25% PMMA; (F) PVDF

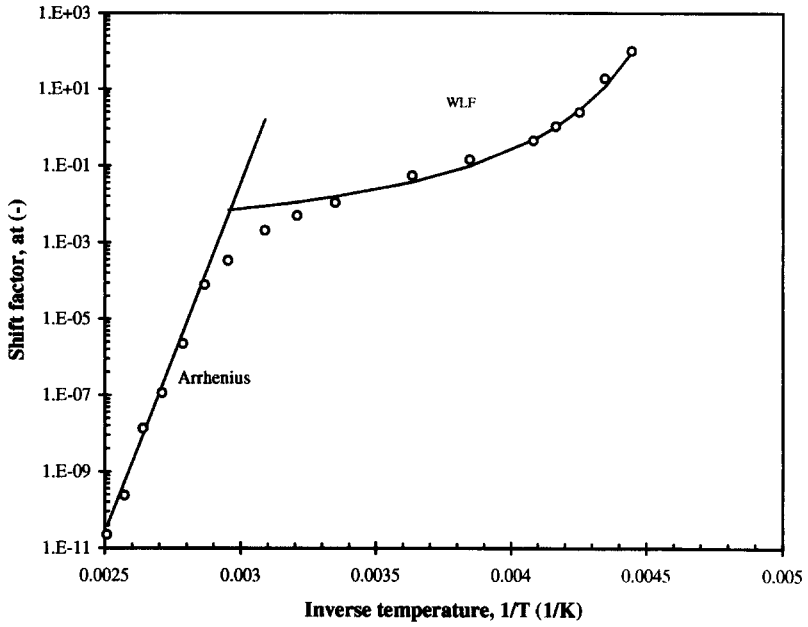

Figure 9 Shift factor as a function of inverse temperature for PVDF showing two regimes

$$(T_g^{PMMA} - T_g^{blend})\cdot\phi_{PMMA} + \kappa\cdot(T_g^{PVDF} - T_g^{blend})\cdot\phi_{PVDF} = 0$$

where κ is $\Delta\alpha_{PVDF}/\Delta\alpha_{PMMA}$ and $\Delta\alpha$'s are the difference between the thermal expansion coefficients below and above the T_g's of the homopolymers[2]. Fitting the data in *Figure 3* to a linear regression yields a value of $\kappa = 0.38$ which is in good agreement with reported values of 0.37–0.4[2,7]. The results for the Gordon–Taylor equation are plotted in *Figure 3*. The actual data starts to deviate from the predicted values at a PVDF concentration of about 40–50 wt%. If it is assumed that the measured value represents the T_g for the amorphous blend in the system, it may be possible to account for this deviation. Hahn *et al.* have reported a phase diagram for extruded blends which was used to improve the prediction of the Gordon–Taylor equation (*Figure 3*). A small deviation was still present, thus, the compositions of the blends were adjusted to give the best fit. The resulting phase diagram for this system is shown in *Figure 14*. For this particular blending technique, one can see the system forms a single amorphous phase until a concentration of ~45 wt% PVDF. A phase separation exists at higher concentrations such that the concentration of PMMA in the amorphous domain remains at about 55 wt% until very high PVDF concentrations. At this point there is a sharp decrease of PMMA in the amorphous domain.

This can be clearly seen in the TEM pictures (*Figures 12 and 13*). The blends containing concentrations of PMMA higher than or equal to 50 wt% PMMA (*Figure 12*) have a gray scale variation. PVDF was the molecule stained by OsO_4 making it appear darker in the TEM. Adding PVDF to PMMA caused a uniform change in the color, with occasional dark spots which are less than 1 μm in diameter. Therefore, one can assume PMMA and PVDF form a miscible blend. At higher concentrations of PVDF, how-

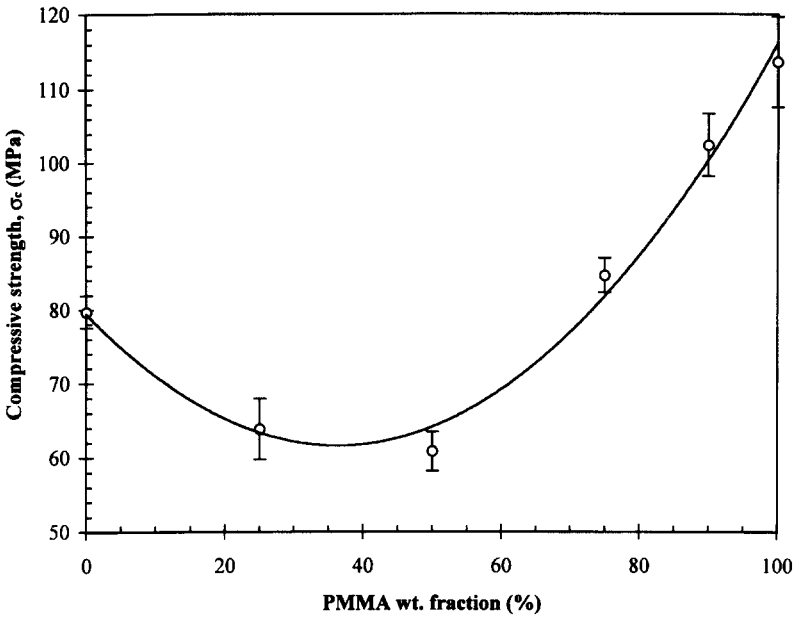

Figure 10 Compressive strength as a function of blend composition

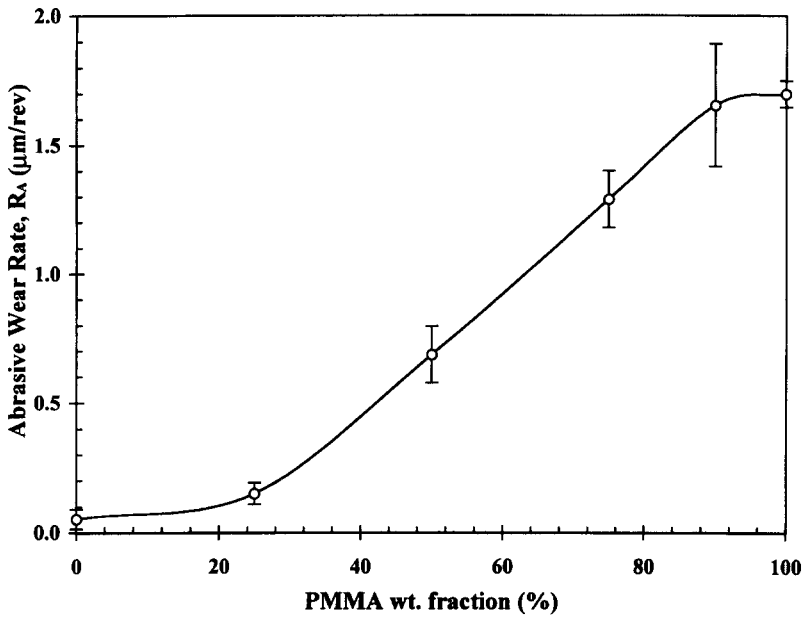

Figure 11 Relative abrasive wear rate as a function of composition

ever, there is a clear phase separation in the system (*Figure 13*). One observes what appears to be the crystalline form of PVDF. The concentration of crystalline domains also increases as the PVDF concentration increases. Thus, the morphological observations indicate good agreement with the phase diagram derived from the T_g data.

Similarly, the phase diagram can be used to evaluate whether other properties may follow the same trend or can be explained by the phase morphology. For instance, several theories have been proposed to calculate the moduli for polymeric blends[17]. One of the simplest forms is similar to the Fox equation:[20]

$$E'_{blend} = \frac{1}{\frac{\phi_{PMMA}}{E'_{PMMA}} + \frac{\phi_{PVDF}}{E'_{PVDF}}}.$$

Figure 15 contains the fit for this equation which shows a deviation at high concentrations of PVDF. By using the values from the phase diagram and again assuming that the observed value is that of the amorphous domain, a better fit is obtained. It seems that a simple relation can be used to describe this system if one takes into account the phase separation. A similar result is found for the flexural strength, where, by taking into account the phase morphology, very close fits are obtained. Of course, it is possible that very different results may be obtained by different processing conditions. However, by annealing the samples, the phase morphology approaches the equilibrium condition where PMMA and PVDF form a single amorphous phase up to ~50 wt% of PVDF[1,2].

There are other material properties where simple correlations cannot be obtained, such as the compressive strength or the abrasive wear rate. In these situations, one can still explain the results by the phase morphology. In the

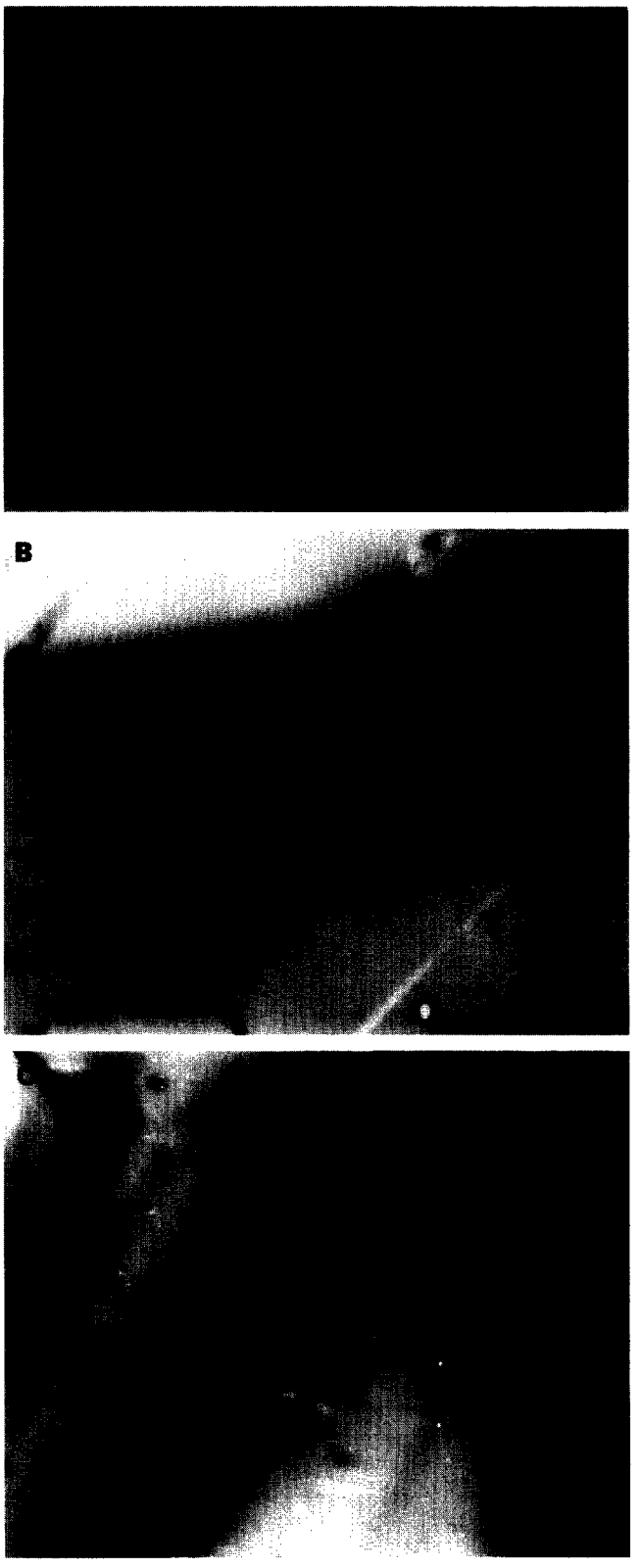

Figure 12 TEM showing homogeneous blends: (A) PMMA; (B) 75% PMMA; (C) 50% PMMA

case of the compressive strength, the blend is completely amorphous at low concentrations of PVDF, and PVDF acts as a plasticiser to reduce the strength of the blend. As the amount of PVDF is increased, the phase separates and crystallises resulting in increasing strength as the crystalline portion of PVDF becomes the principal component[21].

Similarly, the wear of the blends decreases as PVDF is added, caused by the changes in the matrix and the changes

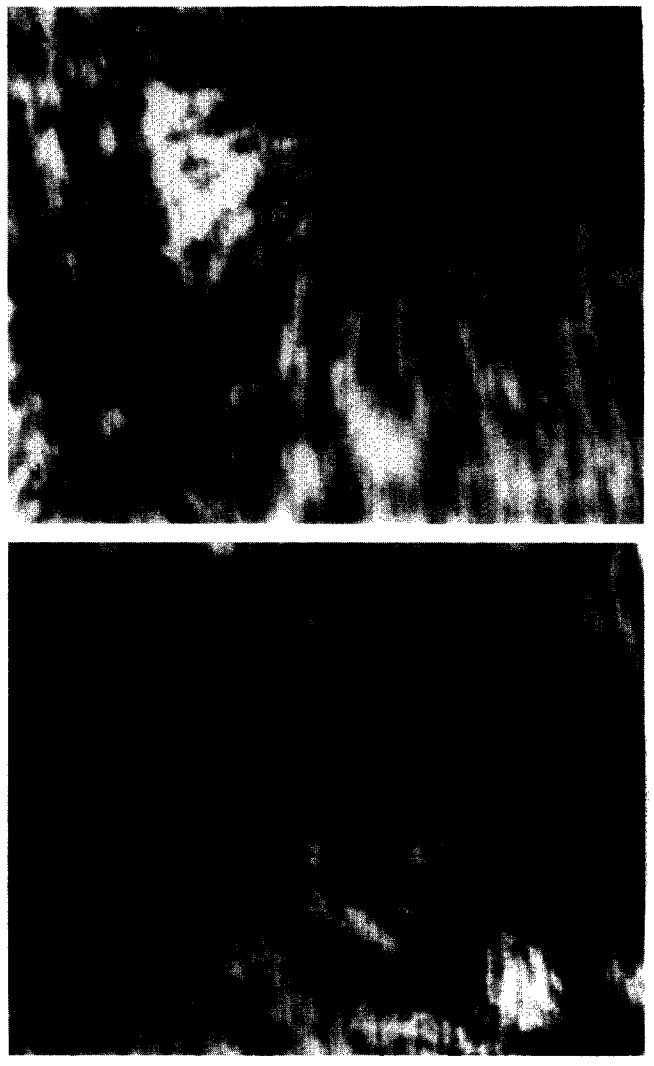

Figure 13 TEM showing crystalline domains: (A) 25% PMMA; (B) PVDF

on the mode of failure. Again, at low PVDF concentrations, the matrix is very brittle and the main mode of failure and wear is by tearing or microcracking resulting in high abrasive wear rates. As more PVDF is added, it plasticises the PMMA and the mode of wear becomes predominantly microcutting, where plastic flow is present, thus reducing the relative wear rate. Finally, when PVDF is present in amounts where phase separation occurs, there are domains of PVDF in the matrix. PVDF itself has a very low coefficient of friction[19] and, therefore, has a very low wear rate in the two-body abrasive system. It seems, then, that the PVDF domains control the wear of the matrix. Further studies are needed, however, to examine both, how these domains are separated, and the composition at the surface.

CONCLUSIONS

The data presented here strongly suggests that the mechanical and wear properties of PMMA/PVDF blends depend on the phase morphology as well as the composition. At low PVDF concentrations, the material is in the form of a single amorphous domain and the properties are those of amorphous blends. When PVDF is present in concentrations higher than 50 wt%, there is a phase separation. The properties of this system seem to be dictated by the predominant domain. At concentrations just above 50 wt%,

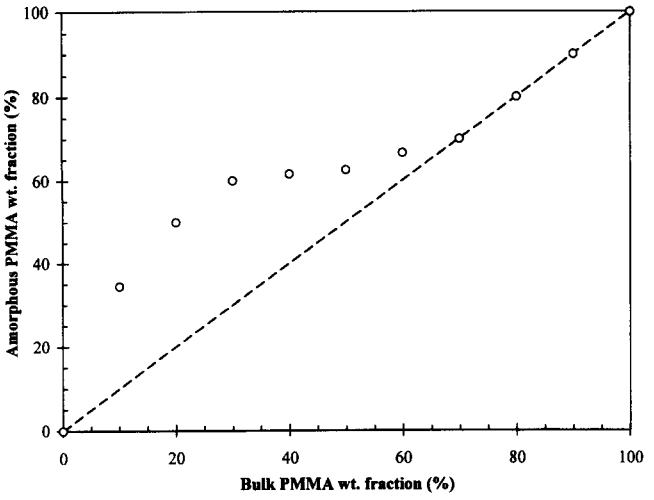

Figure 14 Phase diagram for PMMA/PVDF blends at room temperature

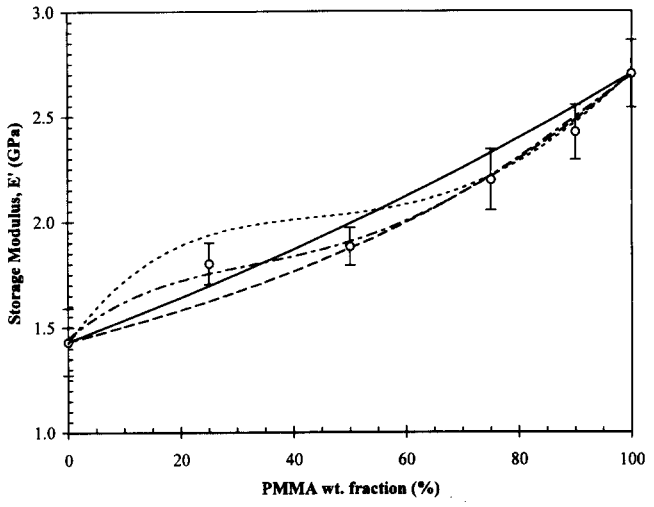

Figure 15 Storage modulus as a function of composition at 10 rad/sec: (E) experimental data; (———) additive rule; (—— ——) Fox-equation fit; (— – —) modified Fox-equation with Hahn *et al.* data[1]; (- - -) modified Fox-equation with data from *Figure 10*

the predominant domain is the amorphous blend with about 50 wt% PVDF and the properties resemble the properties of this amorphous domain. At higher PVDF concentrations the predominant domain is the PVDF domain and the properties are similar to those of pure PVDF.

The range of properties exhibited by the PMMA/PVDF system is similar to the properties of typical materials that are being used as matrices of commercially available dental restorative materials. The major improvement observed was in the area of wear, which is the most common problem with current materials. Thus, this thermoplastic blend system provides an alternative for dental restoratives. Current investigation is ongoing to explore the potential use of this blend system in composites for dental applications.

ACKNOWLEDGEMENTS

This research is funded through the National Institute of Health, Grant No. DE11438.

REFERENCES

1. Hahn, B. R., Herrmann-Schonherr, O. and Wendorff, J. H., *Polymer*, 1987, **28**, 201.
2. Hirata, Y. and Kotaka, T., *Polymer J.*, 1981, **13**, 273.
3. Wang, T. T. and Nishi, T., *Macromolecules*, 1977, **10**, 421.
4. Yang, H., Han, C. D. and Kim, J. K., *Polymer*, 1994, **35**, 1503.
5. Chuang, H. and Han, C. D., *J. Appl. Polym. Sci.*, 1984, **29**, 2205.
6. Kammer, H. W., Kressler, J. and Kummerloewe, C., *Adv. Polym. Sci.*, 1993, **106**, 31.
7. Nishi, T. and Wang, T. T., *Macromolecules*, 1975, **8**, 909.
8. Wu, S., *J. Polym. Sci, Polym. Phys.*, 1987, **25**, 2511.
9. Wolf, M. and Wendorff, J. H., *Polymer*, 1989, **30**, 1524.
10. Wahrmund, D. C., Bernstein, R. E., Barlow, J. W. and Paul, D. R., *Polym. Eng. Sci.*, 1978, **18**, 67.
11. Douglass, D. C. and McBrierty, V. J., *Macromolecules*, 1978, **11**, 766.
12. Martinez-Salazar, J., Camara, J. C. and Calleja, F. J., *J. Mater. Sci.*, 1991, **26**, 2579.
13. Saito, H., Takahasi, M. and Inoue, T., *Macromolecules*, 1991, **24**, 6536.
14. Shimada, S., Hori, Y. and Kashiwabara, H., *Macromolecules*, 1988, **21**, 2107.
15. Siqueira, D. F., Galembeck, F. and Nunes, S. P., *Polymer*, 1991, **32**, 990.
16. Ward, I. M., *Mechanical Properties of Solid Polymers*. Wiley, New York, 1974.
17. Ferry, J. D., *Viscoelastic Properties of Polymers*. Wiley, New York, 1961.
18. Van Krevelen, D. W., *Properties of Polymers*. Elsevier, New York, 1990.
19. Lancaster, J. K., *Encycl. Polym. Sci. Eng.*, 1984, **1**, 1.
20. Dickie, R. A., in *Polymer Blends*, Vol. 1, ed. D. R. Paul and S. Newman. Academic Press, New York, 1978.
21. Paul, D. R., Barlow, J. W. and Keskkula, H., *Encycl. Polym. Sci. Eng.*, 1984, **12**, 399.